Electronic Supplementary Materials

For https://doi.org/10.1631/jzus.A2500404

Two-stage two-dimensional force allocation strategy for tunnel boring machines based on a region-reconfigurable thrust system

Zhe ZHENG[1], Kaihao ZHU[1], Jiaqi HOU[1], Haibo XIE[1], Lijie JIANG[2], Fulong LIN[2], Lianhui JIA[2], Laikuang LIN[3], Huayong YANG[1], Dong HAN[1]

[1]State Key Laboratory of Fluid Power and Mechatronic Systems, School of Mechanical Engineering, Zhejiang University, Hangzhou 310058, China
[2]China Railway Engineering Equipment Group Co., Ltd., Zhengzhou 450047, China
[3]College of Mechanical and Electrical Engineering, Central South University, Changsha 410083, China

S1 Design of region-reconfigurable hydraulic system

The novel region-reconfigurable hydraulic system that comprises 11 PPRVs and 26 TTSDVs is shown in **Fig. S1**. The group configuration can be modified in real time to match the position of the K segment by changing the statuses of these TTSDVs. This eliminates the overturning moment produced by the pressure differentials and maintains a uniform force distribution across all segments. The thrust system of "Linghang" TBM is capable of operating in two modes: full-cylinder independent control and group-based control. Compared with the former one, the region-reconfigurable achieves a nearly 37.5 percent decrease in hardware costs and necessitates 1.6 times fewer control inputs (herein taking the ATOS RZGO PPRVs and the DLEH-3C TTSDVs as references). In contrast to the group-based control, the increased number of TTSDVs considerably improves the capacity to regulate TBM attitude and eliminates the overturning moments. In conclusion, the proposed system strikes a compromise between the hardware cost and the control capability, rendering it technologically practical and economically favourable for the shield tunneling applications.

To further verify the broad application of the region-reconfigurable idea, the thrust system of an additional TBM with an excavation diameter of 14.07 meters is examined. This thrust system is comprised of 17 pairs of hydraulic cylinders, which are assigned to six groups. As illustrated in **Fig. S2**, a whole ring lining comprises one key segment (K), two neighboring segments (L1 and L2), and six standard segments (B1–B6). The region-reconfigurable thrust system is divided into nine groups, and each pair of hydraulic cylinders has three working modes: (1) as a single group, (2) grouped with the adjacent pair on the left, or (3) grouped with the adjacent pair on the right. When the hydraulic system configuration is examined, the following is revealed:

1) Cylinder pairs operating as independent partitions are equipped with two TTSDVs;

2) Cylinder pairs grouped with another pair require three such valves;

3) The valve connection layout follows the same configuration as illustrated in **Fig. S1**.

Therefore, the design principle is summarized as: the number of TTSDVs per group = (the number of hydraulic cylinders per group Times 2) − 1.

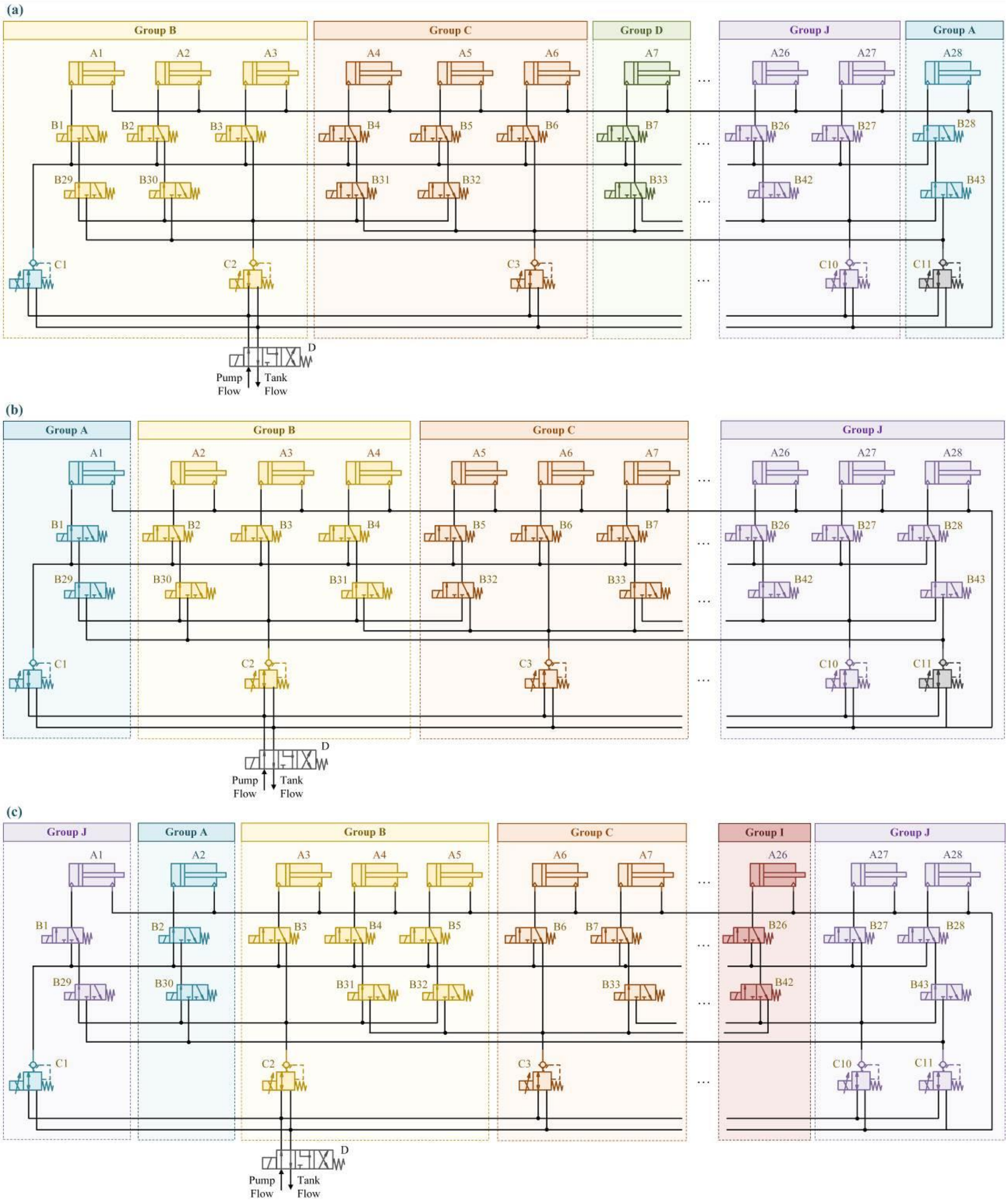

Fig. S1 Hydraulic system configurations corresponding to the installation positions of the K segment: (a) K segment located at cylinder 28; (b) at cylinder 1; (c) at cylinder 2. A1-A28: Hydraulic cylinder; B1-B43: Two-position three-way solenoid directional valves (TTSDVs); C1-C11: PPRVs; D: Three-position four-way solenoid directional valves

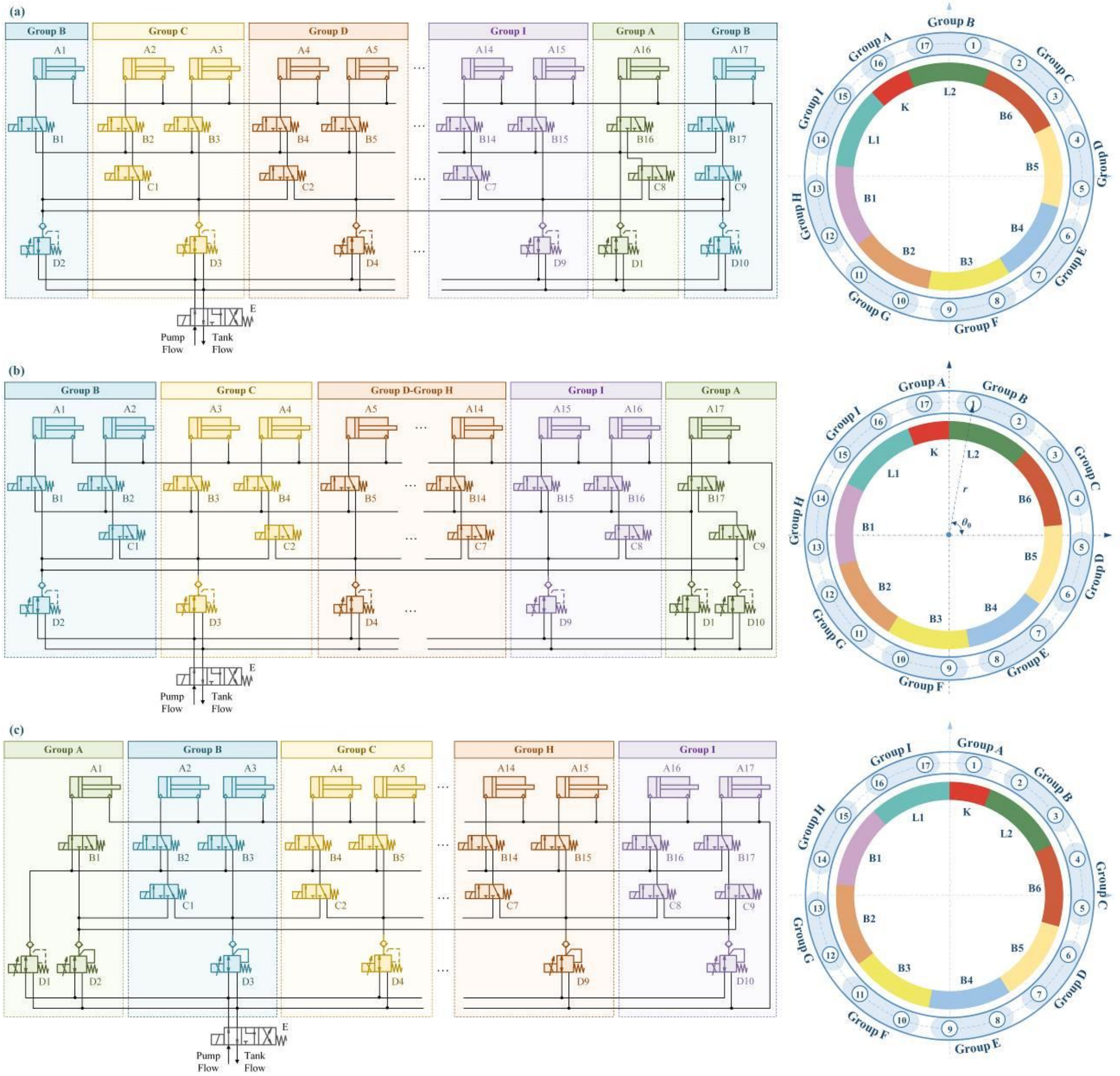

Fig. S2 Hydraulic configurations for the Φ14.07 m thrust system at different assembly positions: (a) K segment located at cylinder 16; (b) at cylinder 17; (c) at cylinder 1. A1-A17: Hydraulic cylinder; B1-C9: TTSDVs; D1-D10: PPRVs; E: Three-position four-way solenoid directional valves

S2 Process of RTNFA

The RTNFA strategy is expressed as:

$$\begin{cases} \boldsymbol{x} = [F_1, F_2, F_3, F_4, F_5, F_6, F_7, F_8, F_9, F_{10}]^{\mathrm{T}} \\ \min \;\; f(\boldsymbol{x}) = \left[f_1(\boldsymbol{x}), f_2(\boldsymbol{x}) \right]^{\mathrm{T}} = \left[J_{\mathrm{TAU}}, J_{\mathrm{TAC}} \right]^{\mathrm{T}} \\ \mathrm{s.t.}\; \boldsymbol{x} \in S = \left\{ \boldsymbol{x} \mid \boldsymbol{x}_{\min} \le g_i(\boldsymbol{x}) \le \boldsymbol{x}_{\max} \right\} \end{cases} \tag{S1}$$

The execution process of NSGA-II can be summarized as follows:

1) A randomly generated initial population of size N is created. The first-generation offspring of size N are generated through genetic operations including selection, crossover, and mutation. The parent and offspring populations are then merged to form a combined population of size $2N$.

2) Non-dominated sorting is adopted on the $2N$ population to determine dominance levels of all individuals, which are ranked based on the Pareto dominance. The top N individuals are selected for the next generation, preserving the best non-dominated fronts until the population size exceeds N. The current set of non-dominated solutions is recorded as L.

3) Crowding distance assignment is carried out within the L_{th} front to measure the density of solutions around a particular individual. Individuals with larger crowding distances are favored to maintain diversity and prevent premature convergence to local optima.

4) The next generation is selected from the sorted population. New offspring are generated via selection, crossover, and mutation operations.

5) Steps 2 - 4 are repeated until a termination condition is met.

The parameter settings for NSGA-II are summarized in **Table S1**. The linprog function is employed to generate an initial feasible population that satisfies the boundary and linear equality constraints, ensuring an unbiased reconstruction of thrust force vector.

The final solution is selected from the generated Pareto set based on the relative importance of objectives under the present tunneling situation. To this end, the technique for order preference by similarity to an ideal solution (TOPSIS) is applied to determine an optimal allocation solution, as it offers the following two advantages (Koohathongsumrit et al., 2021; Wu et al., 2020):

1) TOPSIS evaluates solutions for their proximity to the ideal and anti-ideal, rewarding those that are close to the best and penalizing those that are close to the worst. That is consistent with the engineering requirements for achieving goals and preventing catastrophic consequences.

2) Entropy weighting derives objective weights from the information content of the Pareto set, resulting in objectives with stronger discriminative power receiving a higher weight. This prohibits the arbitrary hand-tuning and the unjust impact of differing units or variations.

Table S1 Parameters of NSGA-II

Variables	Value	Variables	Value
Decision variables	10	Function Tolerance	1e-500
Optimization target number	2	Crossover rate	0.8
Constraints	**Eq. (1)**	Mutation rate	0.7
Initial population number	500	Pareto Fraction	0.8

There are some multi-criteria decision-making (MCDM) techniques widely used in civil engineering, such as analytic hierarchy process (AHP), Vlsekriterijumska optimizacija I kompromisno resenje (VIKOR), or measurement of alternatives and ranking according to compromise solution (MARCOS). The role of AHP is to determine weights based on expert knowledge or preferences, while the alternative ranking is handled by other methods. VIKOR is particularly suitable for explicitly trading off among different criteria, especially when conflicts arise. MARCOS is highly sensitive to normalization results and the magnitude of each criterion, which, in turn, affects the stability and interpretability of the solution ranking. In this paper, J_{TAU} and J_{TAC} do not exhibit intense mutual conflict, and they imply a huge difference in magnitude. Therefore, TOPSIS is better suited to the force allocation problem addressed in this paper. The subsequent paragraphs provide a concise introduction to TOPSIS execution process:

1) Construct an $m \times n$ evaluation matrix, where m is the number of Pareto solutions and n is the number of evaluation indicators.

2) Normalize the evaluation matrix and calculate the weights of the evaluation indicators using the entropy weight method.

$$\begin{cases} E_j = -\dfrac{1}{\ln(m)} \displaystyle\sum_{i=1}^{m} \dfrac{x_{ij} \ln\left(x_{ij}\right)}{\displaystyle\sum_{i=1}^{m} x_{ij} \ln\left(x_{ij}\right)} \\ w_j = \dfrac{1 - E_j}{\displaystyle\sum_{i=1}^{n} \left(1 - E_j\right)} \end{cases} \tag{S2}$$

where x_{ij} is the j-th indicator value of the i-th evaluation scheme, E_j is the information entropy of the j-th indicator, w_j is the weight of the j-th indicator, and $\boldsymbol{X}$ is the weighted standardized evaluation matrix.

3) Set positive ideal solution and negative ideal solution:

$$\begin{cases} \boldsymbol{X}^+ = \left(X_1^+, X_2^+, X_3^+, \cdots, X_n^+\right) \\ \boldsymbol{X}^- = \left(X_1^-, X_2^-, X_3^-, \cdots, X_n^-\right) \end{cases} \tag{S3}$$

4) Calculate the Euclidean distance between the evaluation scheme and the positive ideal solution and the negative ideal solution s_i^+, s_i^-:

$$\begin{cases} s_i^+ = \sqrt{\displaystyle\sum_{j=1}^{n} \left(x_{ij} - X_i^+\right)^2} \\ s_i^- = \sqrt{\displaystyle\sum_{j=1}^{n} \left(x_{ij} - X_i^-\right)^2} \end{cases} \tag{S4}$$

5) Calculate relative closeness

$$D_i = \frac{s_i^-}{s_i^+ + s_i^-} \tag{S5}$$

where D_i is the relative closeness to the ideal solution.

S3 The pseudo-code for the implementation of TSTDFA

Table S2 presents the pseudocode implementation for TSTDFA. When tunneling begins, the segment assembly position is entered to initiate a command that modifies the group layout. Real-time thrust force vectors are gathered, and the force allocation strategy is determined by identifying the tunneling stage. Once TBM finishes the stable stage, the current allocation process is paused for segment installation. Afterwards, the K segment position is updated again, and the execution process proceeds iteratively.

Table S2 Pseudo-code of the execution of TSTDFA

Inputs: The position s of the K segment, thrust force vector v = [F_z, M_x, M_y], advancing speed v
Outputs: The force of each group at the t-th step $\boldsymbol{x}_t$
• **Initialization:**
1. Define thrust system structural parameters: N, n_k, r, θ_0
2. Set parameters for GA and NSGA-II algorithms
• **Execution:**
1. Input s of the current excavation ring
2. Update the group layout of thrust system
3. Initialize allocation step t = 0
4. **function** force_allocation ($\boldsymbol{x}_{\mathbf{prev}}$, v):
When advancing speed v > 0, do
if the tunneling status is in the ramping-up stage, **then**
Execute RSDFA
if exitflag ≤ 0 (indicating no feasible solution) **then**
Execute GLLFO
Return $\boldsymbol{x}$, J_{TAU}
else
Execute RTNFA
Return $\boldsymbol{x}$, J_{TAU}, J_{TAC}
end if
$t = t + 1$

S4 The discussion of convergence properties

In the laboratory tests, we used a desktop workstation equipped with an AMD Ryzen 9 5900X CPU (12 cores). Based on the same dataset, we tested the run times for NSGA-II and the weighted QP. Note that GA-LLS is specifically designed to handle the non-solution cases; therefore, it was tested on another dataset. The convergence of the QP-based solvers directly follows from the problem structure in **Eq. (8)** and **Eq. (14)**, and is therefore not repeated here. For NSGA-II, it is known that when the mutation operator is ergodic and population diversity is maintained, the algorithm asymptotically approximates the Pareto-optimal front. In the implementation, a relatively large population size and number of generations are used, so that NSGA-II is allowed to iterate sufficiently and the resulting Pareto front becomes numerically stable. As for the proposed GA-LLS method, it should be clarified that "convergence" here does not mean convergence to the global optimum of the original QP, because GA-LLS is specifically designed for cases where the feasible set is empty. GA-LLS combines a global stochastic search with a local analytical correction. In each generation, GA generates new candidate group forces, and LLS deterministically adjusts each individual to better satisfy the equilibrium equations and reduce the residual. In this sense, LLS acts as a local improvement operator on the fitness function, while GA provides global exploration capability. In our numerical experiments, we run NSGA-II and GA-LLS 20 times, respectively, and the resulting J_{TAU} and J_{TAC} are identical across runs, with no noticeable discrepancies. This high consistency across independent runs provides strong empirical evidence of the numerical convergence and robustness of the proposed methods. The measured runtimes are reported in **Table S3**. The computational cost of the weighted QP required about 0.05 s per invocation on average; NSGA-II with TOPSIS takes about 19 s, and the GA-LLS takes about 19 s on average. Since the time delay always exceeds half a minute, which is much longer than the average execution period of NSGA-II and GA-LLS. Therefore, we believe that the computational cost can meet the field requirements.

Table S3 Computation time of the proposed methods

Method	Computation time (s)										
	1	2	3	4	5	6	7	8	9	10	Average
QP	0.429	0.015	0.011	0.008	0.042	0.006	0.003	0.002	0.003	0.002	0.052
NSGA-II	27.579	23.120	22.877	21.489	21.739	21.322	21.775	3.979	5.012	21.309	19.020
GA-LLS	14.075	14.980	13.420	14.845	14.205	14.268	15.343	12.963	14.614	12.913	14.163

References

Koohathongsumrit N, Meethom W, 2021. Route selection in multimodal transportation networks: a hybrid multiple criteria decision-making approach. *Journal of Industrial and Production Engineering*, 38 (3), 171-185. https://doi.org/10.1080/21681015.2020.1871084.

Wu B, Lu M, Huang W, et al., 2020. A Case Study on the Construction Optimization Decision Scheme of Urban Subway Tunnel Based on the TOPSIS Method. *KSCE Journal of Civil Engineering*, 24 (11), 3488-3500. https://doi.org/10.1007/s12205-020-1290-9.